Compositional Tuning of Structural Stability of Lithiated Cubic Titania via a Vacancy-Filling Mechanism under High Pressure

Hui Xiong,[1,*,†] Handan Yildirim,[1] Paul Podsiadlo,[1] Jun Zhang,[1] Vitali B. Prakapenka,[2] Jeffrey P. Greeley,[1,‡]
Elena V. Shevchenko,[1] Kirill K. Zhuravlev,[2] Sergey Tkachev,[2]
Subramanian K. R. S. Sankaranarayanan,[1,*] and Tijana Rajh[1,*]

[1]*Center for Nanoscale Materials, Argonne National Laboratory, 9700 S. Cass Avenue, Argonne, Illinois 60439, USA*
[2]*Center for Advanced Radiation Sources, University of Chicago, Chicago, Illinois 60637, USA*
(Received 9 August 2012; published 13 February 2013)

Experimental and theoretical studies on the compositional dependence of stability and compressibility in lithiated cubic titania are presented. The crystalline-to-amorphous phase transition pressure increases monotonically with Li concentration (from ~17.5 GPa for delithiated to no phase transition for fully lithiated cubic titania up to 60 GPa). The associated enhancement in structural stability is postulated to arise from a vacancy filling mechanism in which an applied pressure drives interstitial Li ions to vacancy sites in the oxide interior. The results are of significance for understanding mechanisms of structural response of metal oxide electrode materials at high pressures as well as emerging energy storage technologies utilizing such materials.

PACS numbers: 82.47.Aa, 62.25.−g

Rechargeable Li-ion batteries are pivotal technologies in energy storage, which have found great success in portable electronic devices, and are the leading candidate for powering the next generation hybrid electric and plug-in hybrid vehicles. However, the problems associated with Li-ion battery technology still include safety, degradation, and capacity fade [1]. Insertion and extraction of lithium cause expansion and contraction of active materials. In particular, high cycling rates can induce local points of stress, eventually causing material fracture and capacity fade [2]. High-pressure stability and bulk compressibility directly relate to the response of solids to stress [3], which is the major reason for fractures and pulverization in electrodes. High-pressure methods have been widely utilized to synthesize new electrode materials not achievable under ambient conditions. Several commercially utilized battery materials have been synthesized under high pressure and were optimized for battery applications [4–10]. However, there are only a few studies on the mechanical properties of electrodes under high pressure [11]. A study focusing on compression behavior of electrode materials under high pressure could provide critical insights into their stability and can serve as a guide for battery system optimization.

Titanium dioxide (TiO_2) has a rich phase diagram with many polymorphs that have useful features for Li-ion batteries [12]. TiO_2 is one of a few metal oxide anodes, which intercalate Li ions at a reasonably low potential for safe operation. Whereas rutile and anatase phases of TiO_2 are abundant in nature and extensively used in many industrial applications, cubic TiO_2 is still a desirable material with superior electronic and mechanical properties [13–15]. However, its synthesis is extremely difficult, requiring high temperature (between 1900 and 2100 K)

and high pressure (48 GPa) conditions [13]. Interestingly, we found that cubic TiO_2 can be made as nanotubes under ambient conditions using electrochemical approaches *in operando* [16]. In general, TiO_2 nanotubes are considered as a better electrode material compared to other nanostructured titanias because of their enhanced kinetics [17]. The cubic TiO_2 nanotube anode demonstrates self-improving capacity, high rate capability, and surprising stability ([16]; see Ref. [18] Supplemental Material, Figs. S1 and S2).

Electrochemically prepared cubic TiO_2 has a large concentration of cationic vacancies, which are desirable for electrochemical intercalation of Li ions, but can affect electrode stability. Li intercalation into vacancy sites during electrode cycling can have a twofold effect. The existence of cationic vacancies can cause mechanical instability of crystals [19]. Li intercalation will remove cationic vacancies as Li ions fill vacancies adjacent to reduced Ti centers, hence leading to more robust materials. On the other hand, intercalation of Li ions can cause disorder as ions diffuse through the equilibrated crystalline lattice causing the displacement of the host lattice atoms and eventually leading to amorphization of the material. Which of these scenarios will dominate is dependent on the interplay between the atomic relaxation dynamics in the two processes.

In this Letter we investigate high-pressure stability and compression behavior of cubic $TiO_2(c\text{-}TiO_2)$ phases with Li concentration under a quasihydrostatic condition. *In situ* synchrotron x-ray diffraction (XRD) was investigated up to ~60 GPa [18] (typical pressure limit range for most phase transitions observed for bulk or nano TiO_2 [20,21]) at ambient temperature using the diamond-anvil cell. We have correlated the experimental observations with molecular dynamics (MD) simulations in order to elucidate the role of Li ions in the stability of $c\text{-}TiO_2$. We find that

structural stability of c-TiO$_2$ is enhanced with increasing Li concentration and is explained by a vacancy filling mechanism—an applied pressure drives the interstitial Li ions to the cation vacancy sites in the oxide interior, leading to a significant improvement in structural stability.

We find that the delithiated c-TiO$_2$ nanotube sample (see Supplemental Material for experimental details [18]) is an unexpectedly stable structure (considering the large number of vacancies) that undergoes a pressure-induced amorphization (PIA) above ~17.5 GPa [Fig. 1(a)]. The analysis of the diffraction pattern at ambient pressure indicates highly crystalline material having a cubic phase ($Fd\bar{3}m$) with a cell parameter of 8.22 Å. Increasing the pressure to the range of 7.5–12.0 GPa, we find that all the peaks are shifting monotonically to smaller d spacing along with progressive peak broadening. At the pressure of 17.5 GPa, a significant reduction in the intensity of the (400) reflection was observed, and also the (440) reflection had nearly disappeared, suggesting that disorder starts to settle in the structure. At a pressure above 21.0 GPa, all the diffraction peaks disappeared indicating that a PIA took place in this pressure range. Further compression to 52.8 GPa followed by decompression to the ambient pressure showed that the sample stays disordered. We shall note that although the delithiated c-TiO$_2$ nanotubes have about 50% of vacancies, the PIA occurs at the range of 17.5–21.0 GPa, which is a value similar to those reported for other nanosized TiO$_2$ polymorphs [21–24]. This suggests a surprising stability of delithiated c-TiO$_2$ nanotubes despite the presence of the high concentration of vacancies (~50% cations replaced with vacancies).

High concentration of intercalated Li ions that fill out the majority of the cationic vacancy sites stabilizes the cubic structure. Figures 1(b) and 1(d) show the pressure evolution

of the fully and partially (~75%) lithiated c-TiO$_2$ nanotube at ambient temperature. The starting material is crystalline with the cubic phase ($Fd\bar{3}m$). The cell parameter of the unit cell of fully lithiated c-TiO$_2$ at ambient pressure corresponds to 8.31 Å that is somewhat smaller than the one previously reported for chemically prepared bulk Li$_2$Ti$_2$O$_4$ ($a = 8.376$ Å) [25] of the same symmetry. Geometric optimization using density functional theory calculations gives an optimized lattice constant of 8.27 Å, suggesting a good balance of electrostatic forces in electrochemically synthesized lithiated c-TiO$_2$ [16].

Increasing the pressure up to ~60 GPa of the fully lithiated c-TiO$_2$ nanotubes yielded a progressive decrease of the unit cell parameters to 7.52 Å. Similar behavior was also observed for partially lithiated c-TiO$_2$ (75%). Upon releasing, both samples maintained a cubic structure without undergoing a phase transition as indicated by a smooth monotonic shift of lattice parameters. However, a progressive peak broadening for both lithiated and partially lithiated (75%) samples was observed, suggesting the presence of mechanical stresses from grain-grain interactions induced by compression. The width of the x-ray diffraction peaks narrows as the pressure is restored to the ambient conditions, suggesting that the stress is not permanent, and upon removal of pressure atoms restore their original lattice position.

We performed MD simulations in order to understand the structural response to the applied pressure and the role of Li concentration in the stability of the lithiated and the partially lithiated cubic structures (see Supplemental Material for details [18]). The structural changes at each pressure are analyzed by examining the partial radial distribution functions (PRDFs), which reveal the atomic scale structural changes and the changes in the local bonding
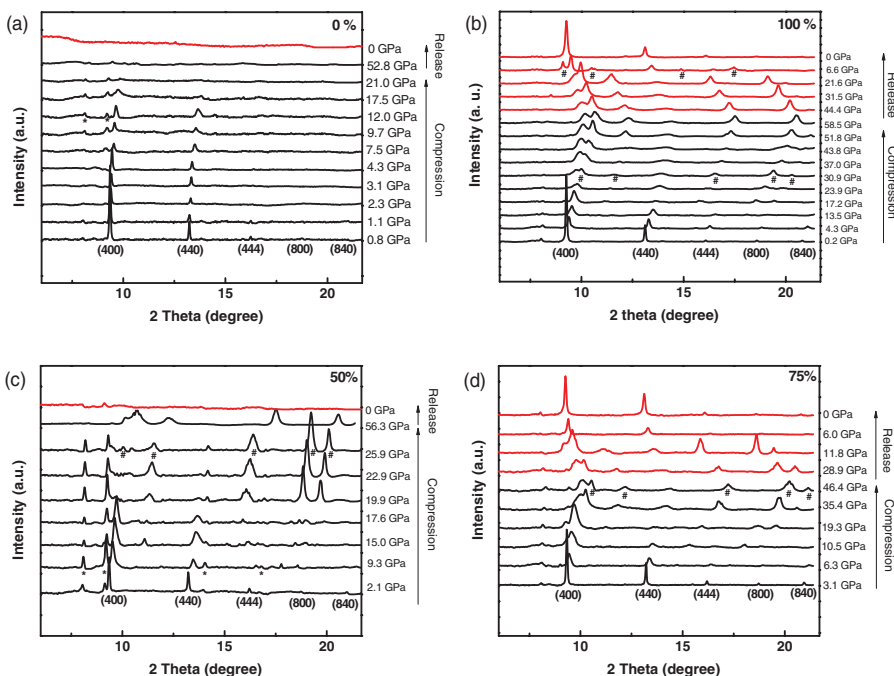

FIG. 1 (color). Integrated *in situ* synchrotron XRD patterns during compression and release of (a) delithiated c-TiO$_2$ nanotubes (0%), (b) lithiated c-TiO$_2$ nanotubes (100%), (c) 50% lithiated c-TiO$_2$ nanotubes, and (d) 75% lithiated c-TiO$_2$ nanotubes. Note that the intensity refinement is not applicable here because of the preferential orientation of TiO$_2$ nanotubes. (Peaks marked by "hash" represent diffraction peaks from unmasked neon, and peaks marked by "asterisk" represent diffraction peaks from unmasked rhenium gasket.)

environment. They indicate the loss of long-range order and a phase transformation at 5 GPa for delithiated c-TiO$_2$. At this pressure, the first nearest-neighbor peak and the bond length distribution become broadened, and the peaks corresponding to higher neighbors become flattened, suggesting that disorder has set in throughout the structure [Fig. 2(a)]. Increasing pressure up to 60 GPa shows that the volume decreases nearly linearly with the pressure and no additional structural transition is observed. In agreement with the experimental data, structural transition obtained by gradually relieving the pressure indicated that the structure remains amorphous.

The results obtained for the fully lithiated c-TiO$_2$, on the other hand, show that the PRDF peak positions related to the first, the second, and higher neighboring shells are shifted toward smaller values revealing the effect of the applied compression, while the width of the peaks remains narrow and well defined [Fig. 2(b)]. This indicates that no significant change is observed in the long-range order as compared to the structure at zero pressure [Fig. 2(b)]. No evidence of phase transition was found for a fully lithiated structure with pressures up to 60 GPa (limit of experimental condition), suggesting a high structural stability of such a structure that is consistent with our experimental observation.

From the MD simulations we constructed P-V plots that suggest no sudden change in the volume for the fully lithiated structure for pressures up to 60 GPa [Fig. 2(c)]. The indication of a phase change can be identified as a sharp break in the P-V plot—the change of the symmetry is accompanied by the abrupt volume change. Similarly, the total energies corresponding to each pressurized structure show a monotonic relation with the pressure, confirming the experimentally observed stability of the fully lithiated

structure. Removing Li from the fully lithiated c-TiO$_2$ introduces cationic vacancies that can change the response of the lattice to an applied pressure. In fact, MD simulation results show a structural transition to an amorphous phase for the 50% Li case [Fig. S3(a) in Supplemental Material [18] and Fig. 2(c)]. Our results also show that the c-TiO$_2$ with 75% Li concentration to be a special one at which we observe the coexistence of two phases (both crystalline and amorphous) at the pressures >35 GPa [Fig. S3(b) in Supplemental Material [18] and Fig. 2(c)]. Below 35 GPa, the pressure-induced volume change is similar to that observed for the fully lithiated structure and maintains its crystallinity. However, for pressures >35 GPa, a slight deviation in the P-V plot is observed, suggesting structural modification. Structural analysis of the simulation trajectories reveals that partial amorphization sets in locally, causing the coexistence of two phases within the structure.

To correlate structural transformations of c-TiO$_2$ with varying Li concentrations as predicted by MD simulations to those of the experimental results, we have constructed an experimental diagram of the unit cell volume changes with applied pressure based on the XRD data (Fig. 3). The experimental P-V data were fitted to the Birch-Murnaghan (B-M) equation of state (EOS) [26] (Supplemental Material [18]). We find that the data for the fully lithiated c-TiO$_2$ follow the EOS fit well. In this case the unit cell could be compressed monotonically to a much smaller volume, reaching at 60 GPa ∼74% of the volume of the ambient pressure. In reverse, during the release of the pressure, the volume follows the same monotonic function and elastically bounces back to the unpressurized unit cell volume indicating reversibility of the nanotube compressibility. The high compressibility of the unit cell is manifested by a low
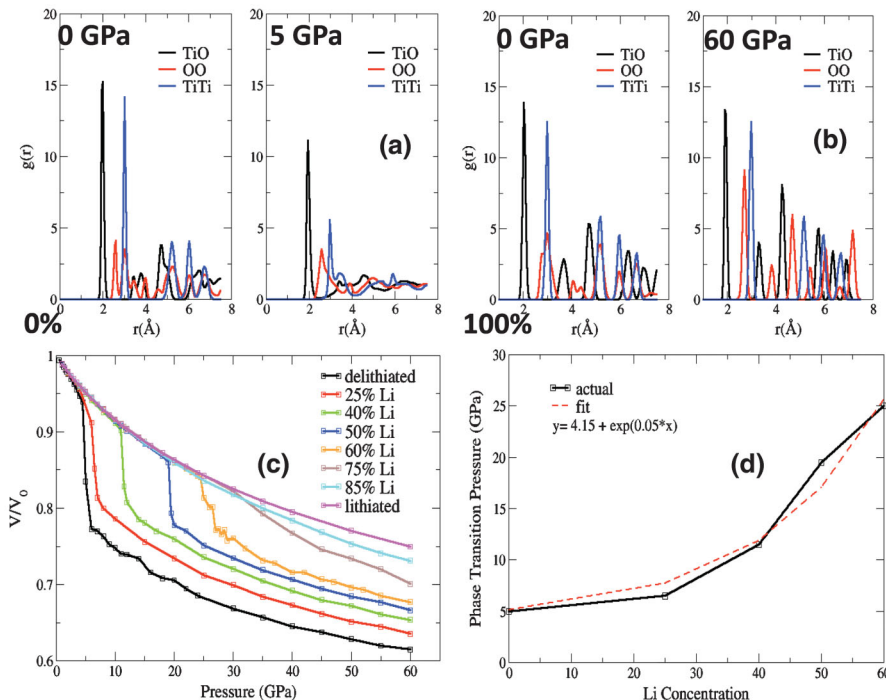

FIG. 2 (color).   (a) Theoretical PRDF of the pairs for the delithiated (0%) cubic TiO$_2$ at 0 and 5 GPa. (b) PRDF of the pairs for the fully lithiated (100%) cubic at 0 and 60 GPa. (c) Volume changes as a function of the pressure for each concentration. (d) Phase transition pressure as a function of Li concentration.
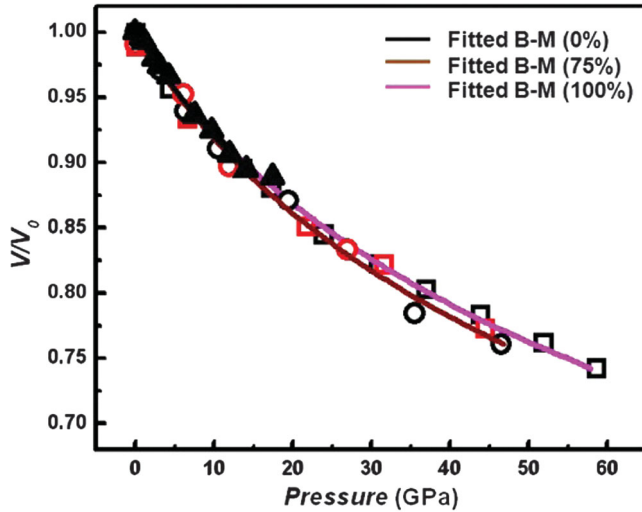
FIG. 3 (color).   Relative unit cell volume changes with pressure in c-TiO_2 nanotubes with different Li concentration based on the data presented in Fig. 1. Solid lines are fitted curves by B-M EOS. Symbols: 0% solid triangles; 75% open circles; 100% open squares. Compression is shown in black, release in red. Error bars are within the symbols.

bulk modulus B_0 of ~100 GPa (Supplemental Material [18]) compared to the nanocrystalline and micro-crystalline anatase of 237 GPa [27] and 179 GPa [28], respectively. Similar to our theoretical considerations of the partially lithiated (~ 75%) TiO_2, we observe a deviation from the EOS fit compared to the fully lithiated c-TiO_2 that is apparent at the pressures >35 GPa. On the other hand, unlike both the lithiated c-TiO_2 and the partially lithiated (~75%) c-TiO_2 nanotubes that maintain their crystallinity (cubic) throughout the compression-decompression cycle, we observe a deviation from the EOS fit consistent with lattice stiffening at 17.5 GPa followed by a complete amorphization of the delithiated sample at ~21 GPa. The enhanced experimental phase transition pressure compared to MD simulations can be attributed to the nano-size effect.

The structural response mechanism to an applied pressure and enhanced stability with increasing Li concentration was elucidated by analyzing the atomistic details of Li ion diffusion in various partially lithiated structures (Fig. 4). The initial minimum energy configurations of the partially lithiated structures are composed of Li ions located at the interstitial sites, leaving cationic vacancies in the cubic oxide lattice. PRDFs (Ti-Ti, Ti-O, and O-O pairs) for the zero pressure configurations at various intermediate concentrations confirm the structural similarity between the oxide lattice in the delithiated and the fully lithiated structures. The main difference introduced by increasing the Li ion concentration in defective cubic titania under high pressures is a decrease in the corresponding number of vacancies owing to migration of interstitially located Li ions to these vacant sites. For the Li concentrations below 75%, we find that increasing pressure leads to a sudden

collapse of the crystallinity of the structure [see the cases for 0 and 50% Li in Figs. 4(a) and 4(b)] above the phase transition pressure, which increases with increasing Li concentration. We find the fully delithiated cubic titania to have the lowest phase transition pressure. Increasing Li concentration from 0 to 75% is found to reduce the number of existing vacancies in the structure. The snapshots shown for 75% lithiated titania in Fig. 4(c) exhibit that increasing pressure forces Li ions to diffuse and fill the vacancies. At this concentration we find that, only above 30 GPa, a slight disorder sets in the structure, occuring fairly gradually rather than abruptly as seen for the concentrations below 75%. The observed enhancement in structural stability with increasing Li concentration to an applied external pressure arises from a vacancy filling mechanism shown schematically in the case of 85% Li [Fig. 4(d)]. The applied pressure drives the interstitial Li ions (shown in green) to the vacancy sites in the oxide interior leading to significant improvement in structural stability. Importantly, the onset of amorphization is a result of the local depletion of Li ions that are necessary to stabilize the vacancy sites. For 85% lithiated titania, a small number of vacancies exist in the structure, and increasing pressure leads to the filling of these vacancies by highly mobile Li ions imparting structural stability against the applied compression. In the fully lithiated case no structural transition is observed [Fig. 4(e)]. These results are the indications of the high pressure structural stability of the Li-rich and the fully
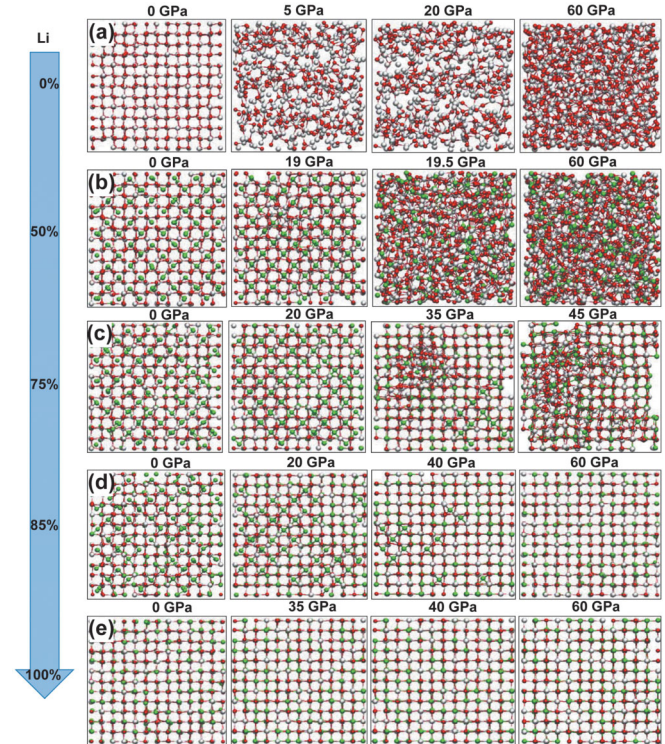

FIG. 4 (color). Structural transition under pressure for (a) delithiated, (b) 50% lithiated, (c) 75% lithiated, (d) 85% lithiated, and (e) fully lithiated at different pressures. Red spheres: O; green spheres: Li; and white spheres: Ti.

lithiated cubic structures, and they are in good qualitative agreement with the experimental observations.

In summary, we observed unusual compression behaviors of lithiated cubic TiO_2 nanotubes by *in situ* XRD and atomistic simulations. While fully lithiated TiO_2 maintains its cubic structure upon compression to ~60 GPa and the subsequent pressure release, delithiated cubic TiO_2 undergoes a PIA at pressure $> \sim 17.5$ GPa and stays amorphous with pressure up to 50 GPa as well as a release to ambient pressure. We show that Li concentration plays a critical role in dictating the stability of the lithiated TiO_2. Our finding suggests that, although surprisingly stable, the c-TiO_2 nanotube electrode is most vulnerable in a discharged state (delithiated). Increased Li concentration gives rise to a vacancy filling mechanism under the applied pressure that enhances the structural stability of cubic TiO_2 by leading interstitial Li ions to the cation vacancy sites. It is important to note that in battery electrodes large atomic rearrangements and high stress are expected at the highest Li concentration gradient. The observed vacancy filling mechanism suggests that the enhanced stability of c-TiO_2 electrodes is a consequence of a pressure initiated ordering at the sites subjected to the highest local stress. These findings could benefit the optimization of battery electrodes and show that high cationic vacancy content in cubic materials assists in accommodating electrode stress and improves their long-term stability for Li-ion battery operation.

---

*Corresponding authors.
clairexiong@boisestate.edu
skrssank@anl.gov
rajh@anl.gov
†Present address: Department of Materials Science and Engineering, Boise State University, 1910 University Drive, Boise, ID 83725, USA.
‡Present address: School of Chemical Engineering, Purdue University, West Lafayette, IN 47907, USA.

[1] J. M. Tarascon and M. Armand, Nature (London) **414,** 359 (2001).
[2] C. K. Chan, H. Peng, G. Liu, K. McIlwrath, X. F. Zhang, R. A. Huggins, and Y. Cui, Nat. Nanotechnol. **3,** 31 (2008).
[3] P. Dera, in *High-Pressure Crystallography: From Fundamental Phenomena to Technological Applications*, edited by E. D. P. Boldyreva (Springer, New York, 2010), p. 1.
[4] C. R. Fell, D. H. Lee, Y. S. Meng, J. M. Gallardo-Amores, E. Morán, and M. E. Arroyo-de Dompablo, Energy Environ. Sci. **5,** 6214 (2012).
[5] R. Stoyanova, E. Zhecheva, R. Alcántara, J. L. Tirado, G. Bromiley, F. Bromiley, and T. B. Ballaran, Solid State Ionics **161,** 197 (2003).
[6] M. Yoncheva, R. Stoyanova, E. Zhecheva, R. Alcántara, G. Ortiz, and J. L. Tirado, J. Solid State Chem. **180,** 1816 (2007).
[7] M. E. A. de Dompablo, J. M. Gallardo-Amores, U. Amador, and E. Morán, Electrochem. Comm. **9,** 1305 (2007).
[8] J. M. Gallardo-Amores, N. Biskup, U. Amador, K. Persson, G. Ceder, E. Morán, and M. E. A. de Dompablo, Chem. Mater. **19,** 5262 (2007).
[9] O. Garcã-a-Moreno, M. Alvarez-Vega, J. García-Jaca, J. M. Gallardo-Amores, M. L. Sanjuán, and U. Amador, Chem. Mater. **13,** 1570 (2001).
[10] B. Voã Ÿ, J. Nordmann, A. Kockmann, J. Piezonka, M. Haase, D. H. Taffa, and L. Walder, Chem. Mater. **24,** 633 (2012).
[11] Y. Lin, Y. Yang, H. Ma, Y. Cui, and W. L. Mao, J. Phys. Chem. C **115,** 9844 (2011).
[12] Z. G. Yang, D. Choi, S. Kerisit, K. M. Rosso, D. Wang, J. Zhang, G. Graff, and J. Liu, J. Power Sources **192,** 588 (2009).
[13] M. Mattesini, J. S. de Almeida, L. Dubrovinsky, N. Dubrovinskaia, B. Johansson, and R. Ahuja, Phys. Rev. B **70,** 212101 (2004).
[14] Y. Liang, B. Zhang, and J. Zhao, Phys. Rev. B **77,** 094126 (2008).
[15] D. Y. Kim, J. S. de Almeida, L. Koci, and R. Ahuja, Appl. Phys. Lett. **90,** 171903 (2007).
[16] H. Xiong *et al.*, J. Phys. Chem. C **116,** 3181 (2012).
[17] G. Armstrong, A. R. Armstrong, J. Canales, and P. G. Bruce, Chem. Commun. (Cambridge) 19 (2005) 2454.
[18] See Supplemental Material at http://link.aps.org/supplemental/10.1103/PhysRevLett.110.078304 for materials and methods.
[19] L. K. Moleko and H. R. Glyde, Phys. Rev. B **30,** 4215 (1984).
[20] V. Swamy, E. Holbig, L. S. Dubrovinsky, V. Prakapenka, and B. C. Muddle, J. Phys. Chem. Solids **69,** 2332 (2008).
[21] V. Swamy, A. Kuznetsov, L. Dubrovinsky, P. McMillan, V. Prakapenka, G. Shen, and B. Muddle, Phys. Rev. Lett. **96** 135702 (2006).
[22] V. Swamy, A. Kuznetsov, L. Dubrovinsky, A. Kurnosov, and V. Prakapenka, Phys. Rev. Lett. **103** 075505 (2009).
[23] Q. Li *et al.*, J. Phys. Chem. Lett. **1,** 309 (2010).
[24] J. S. Olsen, L. Gerward, and J. Z. Jiang, High Press. Res. **22,** 385 (2002).
[25] R. J. Cava, D. W. Murphy, S. Zahurak, A. Santoro, and R. S. Roth, J. Solid State Chem. **53,** 64 (1984).
[26] F. Birch, J. Appl. Phys. **9,** 279 (1938).
[27] V. Pischedda, G. Hearne, A. Dawe, and J. Lowther, Phys. Rev. Lett. **96** 035509 (2006).
[28] T. Arlt, M. Bermejo, M. Blanco, L. Gerward, J. Jiang, J. S. Olsen, and J. Recio, Phys. Rev. B **61,** 14414 (2000).